Hydrodynamics of Soil Immobilization in the Immobilized Soil Bioreactor

Dimitar G. Karamanev, Claude Chavarie, and Réjean Samson
Industrial Chair on Site Bioremediation, Dept. of Chemical Engineering, Ecole Polytechnique, Montreal, Canada H3C 3A7

The hydrodynamic characteristics of a new type of reactor, the immobilized soil bioreactor, were studied. This apparatus is a practical new engineering concept (soil immobilization) based on entrapment of soil particles, which contain pollutant-degrading microorganisms, in the pores of a geotextile to activate the indigenous microorganisms. The soil immobilization is the third on the size scale of immobilization processes, coming after (1) that of molecules in heterogeneous catalysis (in Angstrom) and (2) that of microbial cells and their fragments in immobilized cells and enzymes biocatalysis (in micron). The size of immobilized soil particles is in the range of a millimeter. A mathematical model of liquid flow within the reactor is proposed, which qualitatively explains the distribution of the immobilized soil in space. The dynamics of soil immobilization within the bioreactor has been studied as a function of the particle size, initial slurry concentration and air flow rate. A mathematical model of the process of soil immobilization was proposed based on deep filter mechanics. The process can be described by a second-order kinetic model. This study will be of great importance for the design of immobilized soil bioreactors for degradation of recalcitrant soil pollutants.

Introduction

Many toxic and recalcitrant chemicals, such as DDT, polychlorinated biphenils (PCBs), pentachlorophenol (PCP), used in the human practice, have been released into the environment and polluted the soil and groundwater (Atlas, 1995). One of the effective ways of treating contaminated soils is soil washing. The biological removal of pollutants from the process water is considered to be one of the limiting steps of the process (EPA, 1992). The biological treatment of contaminants dissolved in groundwater is also an important approach for environmental protection. Therefore, there is a great need for new, highly effective bioprocesses for degradation of recalcitrant pollutants dissolved in water.

It has been shown that soil particles, polluted with a certain recalcitrant organic, often contain a microbial consortium capable of degrading it (Otte et al., 1994; Alexander, 1994). These soil particles can not only be used as a source for developing a microbial consortium for biodegradation but can also serve as a support for the biofilm of this consortium.

In order to activate the microbial consortium present in contaminated soil, the soil particles should be fixed in space to minimize the friction between them and to prevent the particles from leaving the reactor. Furthermore, using chemical adhesives to attach the particles to a soil surface is not recommended, since these adhesives can be harmful to the microorganisms. Therefore, a mechanical method for attaching the soil particles (with a size distribution usually between 10 and 1,000 μm) should be found.

Recently, a new modification of an airlift reactor has been proposed (Karamanev et al., 1996a). The draft tube of this reactor is porous (average pore size between 100 and 200 μm) and is semipermeable. Because the pores are small, the liquid can flow through the draft tube while gas bubbles cannot. It has been found that the liquid flow structure in this reactor is quite unusual compared to classic airlifts. In addition to the vertical flow (upwards in the riser and downwards in the downcomer), the liquid flows horizontally through the draft tube. This flow structure is appropriate for the process of attaching soil particles to a static support. The first application of this bioreactor for pentachlorophenol mineralization was very promising: a volumetric efficiency of up to 900 mg-PCP/L·h was achieved (Karamanev et al., 1996b) which is 1 to 3 orders of magnitude higher than any data on biodegradation of PCP reported in literature. However, the hydrodynamics of the process of attaching soil particles to a static

Correspondence concerning this article should be addressed to D. G. Karamanev.

support within the bioreactor with a semipermeable draft tube has not been characterized.

The goal of this work is to study the hydrodynamics of the process of fixation of various sizes of soil particles into a porous static support in the airlift reactor with a semipermeable draft tube. The results will be of importance in using this apparatus as a bioreactor for the highly efficient treatment of recalcitrant soil pollutants.

Immobilized Soil Reactor

The process of soil particle fixation was studied in the apparatus shown in Figure 1. This apparatus is an airlift reactor with a draft tube made of nonwoven geotextile. The nonwoven geotextile is a highly porous material. Since this material has a wide pore size distribution—between several microns and approximately 300 μm (Silva and Bhatia, 1993; Rigo et al., 1990)—it is expected that different-sized soil particles could be entrapped in these pores, and therefore be fixed in space. (Strictly speaking, nonwoven geotextile has no pores with a determined length and diameter such as are in rigid porous materials like the ones used in catalysis. Rather there are curly fibers in a three-dimensional orientation. Therefore, pore-size distribution cannot be determined quantitatively; the main pore parameter in geotextile is the apparent opening size of filtration.) We called the entrapment process *soil immobilization*, and the apparatus in which it was carried out the *immobilized soil bioreactor*. The soil was immobilized as follows: when the space within the draft tube (riser) is aerated, the difference of the hydrostatic head between both sides of the geotextile causes the liquid in the reactor to circulate. The liquid moves upward in the aerated section, downward in the unaerated section, and horizontally through the geotextile from the unaerated to the aerated zone. The typical liquid flow paths are shown in Figure 1. If the liquid contains suspended soil particles, these can become trapped in the pores of the geotextile when the slurry passes through it. Several different possible mechanisms of entrapment are discussed later.

Mechanisms of Soil Immobilization

The process of particle retaining by nonwoven geotextile is similar to deep bed filtration, where the pore size of the filter is larger than the particle size (Ives, 1970). In this case, the particles are deposited on the surface of the filter material as a result of the following forces: electrostatic, van der Waals forces, mutual adsorption, and straining. Since the range of most of these forces is very small—sometimes below a micron—the particles first have to be transported from the fluid bulk (in the pore space) to the surface of the filter material. The transport mechanisms include diffusion, mechanical inertia, interception, and sedimentation. Since particle retention in deep filtration is a stochastic process (Hsu and Fan, 1984), a higher degree of particle removal can be obtained by increasing the retention time of the contact, usually by increasing the depth of the filter, which is where the term *deep-bed filtration* comes from. Liquids are usually filtered by using a bed of granular filter material, such as sand or carbon, while fibrous materials are usually applied to aerosol filtration (Orr, 1987).

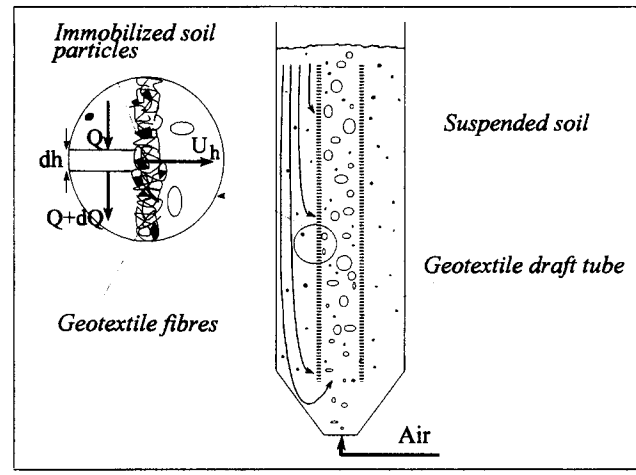

Figure 1. Immobilized soil bioreactor.

Since soil immobilization is a process of retaining particles in pores with a size larger or equal to the pore, it can be described by deep-bed filtration models.

The process of deep-bed filtration of liquids using a filter bed that consists of spherical particles has been fairly well studied. It is mainly used for water treatment (Tien and Payatakes, 1979). The gas filtration by nonwoven fiber materials is also well understood because of its application in aerosol filtration. One of the main uses of geotextiles in geotechnology is to support layers of soil in order to avoid washing. Consequently, the separation of soil particles from a soil–water suspension has been the subject of numerous studies (Christopher and Fischer, 1992). Unfortunately, the process of trapping soil particles in geotextile pores has not been investigated thoroughly.

Mathematical Model of Liquid Flow in the Reactor

Since the liquid flow structure in the reactor is of great importance for the process of soil immobilization, a simple model for predicting the liquid velocity profiles is presented next. A bioreactor without soil particles (gas–liquid system) is considered in this section.

The liquid circulation trajectories within the reactor are shown in Figure 1. In order to consider the flow of liquid through the draft tube wall, the model is based on the case when the geotextile wall is attached to the bottom of the reactor, that is, the bottom clearance is zero. The following assumptions were made:

1. The limiting friction loss is due to the passage of liquid through the wall, that is, the friction in the aerated section (riser), in the unaerated section (downcomer), in the top connecting section, and in all the other losses are insignificant. This assumption was confirmed by Chisti (1989);
2. The flow through the wall is laminar (Darcy flow);
3. The gas holdup in the riser is constant along both the vertical and horizontal coordinates. The gas holdup in the downcomer was assumed to be zero.

Let us consider the flow gradient through the horizontal slice of the downcomer with a height equal to *dh* (Figure 1). The change in the liquid flow rate within the vertical coordinate of the slice is equal to

$$(Q + dQ) - Q = dQ = \psi dS \frac{\Delta p}{\rho g}, \tag{1}$$

where dS is the surface of the geotextile wall contacting the slice of downcomer section, $dS = \pi D_D \cdot dh$; D_D is the draft tube diameter; D_R is the reactor diameter; dQ is the liquid flow through the geotextile with a surface area dS; Δp is the hydrostatic pressure difference between the downcomer and riser at the vertical coordinate h($h = 0$ at the bottom of the geotextile wall); ψ is the permittivity of the geotextile defined as (ASTM, 1992):

$$\psi = \frac{K}{\delta} \tag{2}$$

where K is the coefficient of permeability and δ is the geotextile thickness. Assuming that the gas holdup in the downcomer is zero, the pressure drop can be expressed as

$$\Delta p = \rho g (H_D - h) \epsilon_R \tag{3}$$

where H_D is the height of the draft tube and ϵ_R is the gas holdup in the draft tube. Taking into account that the vertical velocity in the downcomer $U_v = dQ/[\pi(D_D^2 - D_R^2)/4)]$ and combining Eqs. 1 and 3, one can obtain

$$\frac{dU_v}{dh} = 4\psi\epsilon_D \frac{(H_D - h)}{\frac{D_D^2}{D_R} - D_R}. \tag{4}$$

After integrating Eq. 4 (limits: h from 0 to h, and U_v from 0 to U_v), the profile of the vertical component of liquid velocity in the riser (U_v) as a function of the reactor height will be described by

$$U_v = -\frac{2\psi\epsilon_R}{\frac{D_D^2}{D_R} - D_R}\left[(H_D - h)^2 - H_D^2\right] = \frac{2\psi\epsilon_R h}{\frac{D_D^2}{D_R} - D_R}(2H_D - h). \tag{5}$$

Equation 5 shows that the vertical velocity is maximal at the top of the reactor and decreases to zero at the bottom of the reactor. The superficial horizontal liquid velocity can be obtained by combining and rearranging of Eqs. 1 and 3:

$$\frac{dQ}{dS} = U_h = \psi\epsilon_R(H_D - h). \tag{6}$$

Therefore, the liquid velocity in the horizontal direction decreases linearly by h from $U_h = \psi\epsilon_R H_D$ to $U_h = 0$. The profiles of the vertical (Eq. 5) and horizontal (Eq. 6) components of the liquid velocity in the downcomer as a function of the reactor height are shown in Figure 2. The gas holdup in Eqs. 5 and 6 was calculated using the Hills (1976) correlation:

$$\epsilon_R = \frac{U_{GR}}{0.24 + 1.35(U_{GR} + U_{LR})^{0.93}}. \tag{7}$$

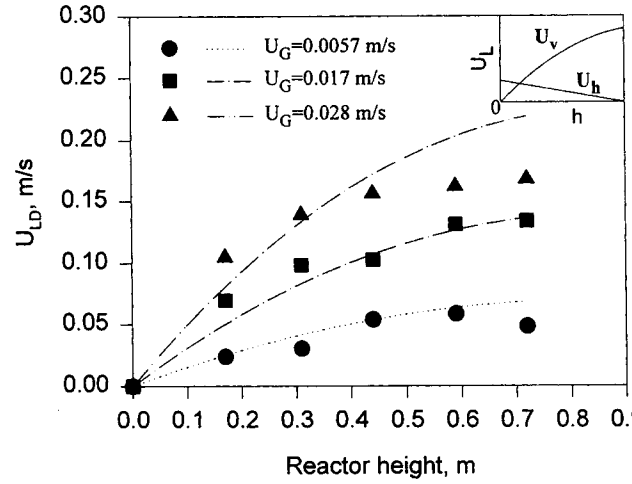

Figure 2. Experimental vs. theoretical liquid-velocity profiles by the reactor height.

Insert: Typical profiles of the horizontal (U_h) and vertical (U_v) components of liquid velocity.

The liquid velocity in the riser (U_{LR}) in Eq. 7 was chosen as the velocity averaged over the height of the draft tube. The permittivity of the geotextile was 1.7 s^{-1}. In Figure 2 the theoretical results are compared with published experimental data for liquid velocity in the vertical direction (Karamanev et al., 1996a). It can be seen that the experimental liquid velocity agrees with that calculated by Eq. 5 only at gas velocities below 0.02 m/s. At higher velocities, the model precisely predicts the experimental data only at the lower part of the bioreactor ($h < 0.5$ m). The liquid velocity is smaller than predicted at the upper half of the reactor. These differences can be explained by the strong increase of the vertical liquid velocity at the top of the reactor. At high velocities, the first assumption is not fully satisfied since there are also significant liquid friction losses in both the riser and the separator (because the direction of the flow changes by 180°). Therefore, the model presented earlier can be used to predict liquid velocities in the reactor in most of the practical cases except when the gas velocity is high.

Experimental Study of Soil Immobilization

Materials and methods

The bioreactor used (Figure 1) was a vertical plexiglass cylinder with an internal diameter of 15 cm and a height of 2 m. The bottom of the reactor was conical. Air was introduced through a perforated disk (1 cm in diameter) mounted at the bottom of the conical section in order to avoid the settling of the soil particles. The draft tube was made of nonwoven geotextile (Texel Co., stock #400 PE 100 A1) supported by a cylindrical stainless-steel grid. The draft tube was 100 cm high, and its internal diameter was 7.5 cm. The air flow rate was measured by a calibrated rotameter.

The solid phase in the experiments was silica sand that was sieved and separated into the following fractions: 0–75 μm, 75–150 μm, 150–250 μm, and 250–400 μm. The experiments for soil immobilization were performed with each of the individual fractions.

The concentration of the suspended particles was measured by separating the solids from the liquid, and then drying and weighing of the particles. The smaller fractions (below 150 μm) were separated by centrifugation at 10,000 rpm ($8{,}000 \times g$ relative centrifugal force), while the larger fractions were separated by settling.

The surface density of soil trapped in the geotextile was measured by the following method. The geotextile of the draft tube was cut vertically into four pieces, which were attached tightly to each other. After the soil immobilization experiment, each of the geotextile pieces was gently detached from the stainless-steel grid supporting it. The immobilized solid particles were removed by a strong water jet. The effectiveness of detachment was over 95%, and was determined from the material balance of solids. The quantity of solids was determined by the volume of settled particles. It was found that this volume was very well correlated to the dry-particle mass.

The experiments for studying soil immobilization were conducted as follows. The reactor was filled with tap water and aeration started. After several minutes, the amount of time necessary to develop steady-state hydrodynamic conditions, a certain volume of silica sand was introduced to the reactor. The concentration of solids in the liquid–solid slurry in the reactor was then followed as a function of time. At the end of the experiment, the vertical profile of the surface density of solids trapped in the geotextile was determined.

The permeability of geotextile containing immobilized soil was studied in a vertical glass tube with an internal diameter of 5 cm and a height of 40 cm. A piece of geotextile was attached to the bottom of the tube and tap water was introduced through a glass tube above the geotextile. The height of water above the geotextile was kept constant (5 cm) by varying the water flow rate. The geotextile permeability was calculated from this flow rate. A certain number of particles were periodically added to the water above the geotextile and the new permeability was measured.

Experimental results

The effect of particle size on the process of soil immobilization was studied next. The same initial concentration of solids was used in each of these experiments. The experimental conditions of each experiment are shown in Table 1. The change in solids concentration in the liquid phase is shown in Figure 3a. It can be seen that the rate of immobilization is at its fastest when the particle size is between 150 and 250 μm. It decreases when increasing or decreasing the size of the particle. The profiles of the surface-soil density by the height of the reactor are shown in Figure 3b. The results for the different particle sizes are close to and within experimental error. Therefore, the vertical profile of the mass of immobilized soil is independent of the particle size. No results for particle size below 75 μm are available because of technical difficulties encountered when trying to measure the surface density (because of the low attachment force at this particle size, it was impossible to remove the geotextile with immobilized soil from water without losing some soil from it). The surface density profile of immobilized soil by the height of the reactor was not exactly linear, but its shape was still similar to that representing the horizontal vector of the liquid velocity profile by the height of the reactor (Figure 2). Therefore, the horizontal velocity of liquid flowing through the geotextile correlates to the quantity of immobilized soil. As a first approximation, one can assume that the surface density of immobilized soil at a certain height is proportional to the liquid velocity through the geotextile at the same point.

Table 1. Calculated Values of the Coefficients λ_0 and β (Eq. 13)

No.	d_p μm	Init. Soil Conc. kg/m^3	Air Vel. m/s	λ_0 s^{-1}	β
1	0–75	11	0.015	0.00215	2.73
2	75–150	11	0.015	0.242	1.42
3	150–250	11	0.015	7.02	1.01
4	250–400	11	0.015	2.52	1.07
5	150–250	3.9	0.015	20.1	0.997
6	150–250	7.9	0.015	17.8	1.00
7	150–250	15.8	0.015	11.0	1.01
8	150–250	23.7	0.015	2.86	1.01
9	150–250	11	0.0075	27.6	0.997
10	150–250	11	0.030	18.7	1.00

The effect of particle size on the total mass of immobilized soil is shown in Figure 4. A strong dependence between these parameters is observed, and as already mentioned, maximal soil immobilization is observed for a particle sizes between 150 and 250 μm. This result can be explained by relating

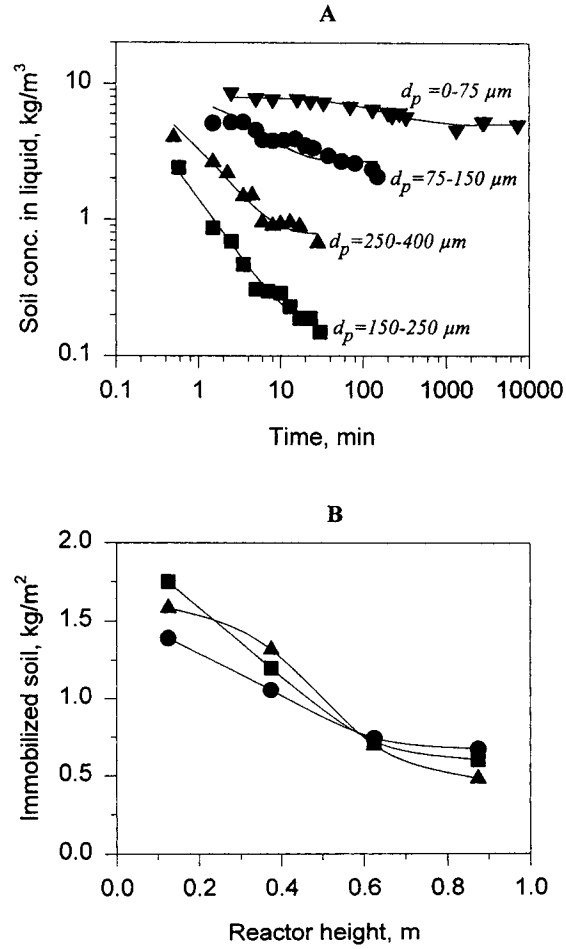

Figure 3. Suspended soil concentration and surface soil density as a function of the particle size.

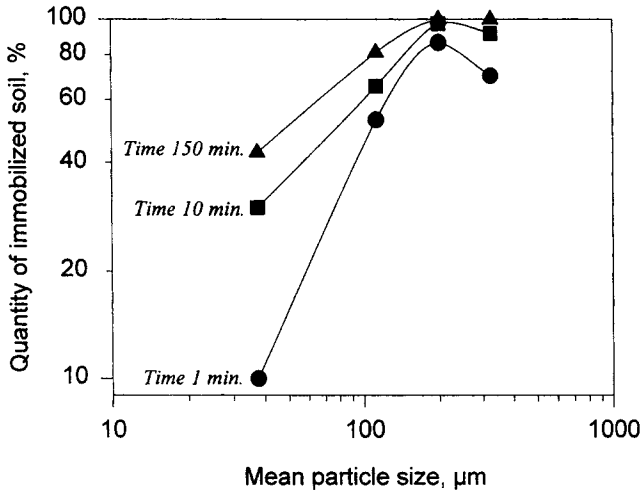

Figure 4. Effect of the particle size on the efficiency of soil immobilization.

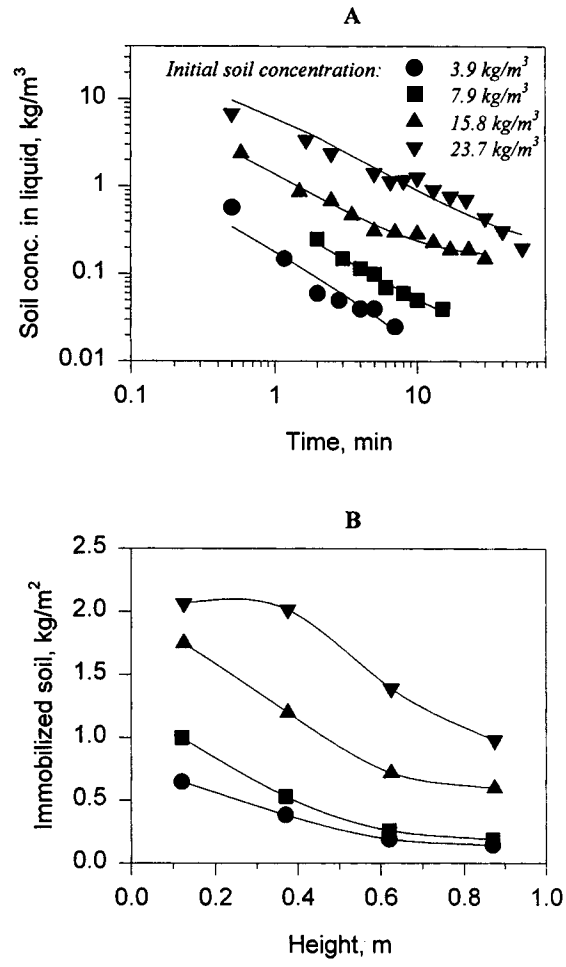

Figure 5. Effect of the initial suspended soil concentration on the process of immobilization.

particle size to the geotextile pore-size distribution. If one assumes that the pore-size distribution curve in the geotextile has a maximum of around 150–250 μm, then particles of the same size will be trapped quicker than other particles.

The soil immobilization process was also studied by varying the initial quantity of solids introduced to the system. The particle size in all these experiments was between 150 and 250 μm (experiments 5–8 in Table 1). The change of the suspended solids concentration with time is shown in Figure 5a. Since all the lines are almost parallel, the process mechanism should be the same at the different initial soil concentrations. More detailed consideration of the mechanism of soil immobilization is made in the following section. The mass of immobilized soil as a function of the height of the reactor is presented in Figure 5b. For surface solids density below 2.0 kg/m^2, the density of the solids decreases along the vertical coordinate. When the density of the solids reached 2.0 kg/m^2 (at the lower 40 cm when the initial solids concentration was 23.7 kg/m^3), however, a plateau can be observed. This can be explained by the saturation of the geotextile with solid particles. Visual observation of the draft tube confirmed this explanation: the solid particles "flowed" down over the external draft tube surface at the lower part of the draft tube at an initial solids concentration of 23.7 kg/m^3. Otherwise, no such effect was observed. Therefore, the maximal quantity of soil fraction between 150 and 250 μm that can be immobilized in the geotextile used is 2.0 kg/m^2.

The effect of the air flow rate on the process of soil immobilization was also studied. Figure 6a shows that this effect is relatively weak: doubling of the air flow rate leads to an approximately 50% increase in the immobilization rate. The profiles of the solids surface density were similar (Figure 6b).

The filtration characteristics of the geotextile used were also studied. First, a dry sieving of silica particles with different size fraction was performed. It can be seen (Figure 7) that almost all 325-μm particles are retained in the geotextile while only a small amount is retained at a particle size below 100 μm. The situation was very different during wet filtration. Filtration was much more effective, especially for 100–200-μm particles. Similar results were reported by Falyse et al. (1985). We can conclude that viscous forces play an important role in the liquid filtration of soil through geotextile. Our results also suggest that the maximal pore size of the geotextile used is around 300 μm.

The permeability of geotextile as a function of the surface soil density was studied next. The relationship between the pressure drop, porosity, and fluid velocity of a laminar flow through a porous medium can be described by the Blake-Kozeny equation (Bird et al., 1960):

$$\frac{\Delta p}{\delta} = 4.17 \mu U_L \left(\frac{S}{V}\right)^2 \frac{(1-\epsilon)^2}{\epsilon^3} \tag{8}$$

where δ is the thickness of the porous bed (in our case geotextile); ϵ is its porosity (calculated from the solid holdup of both geotextile and soil), μ is the liquid viscosity; and (S/V) is the surface to volume ratio of solids in the bed. It can be shown that during the process of soil immobilization, the ratio (S/V) of the system remains constant. Therefore, the liquid velocity through the immobilized soil bed should be proportional to the complex $\epsilon^3/(1-\epsilon)^2$ at constant Δp. That is why the experimental data in this section are presented as a plot between U_L and $\epsilon^3/(1-\epsilon)^2$.

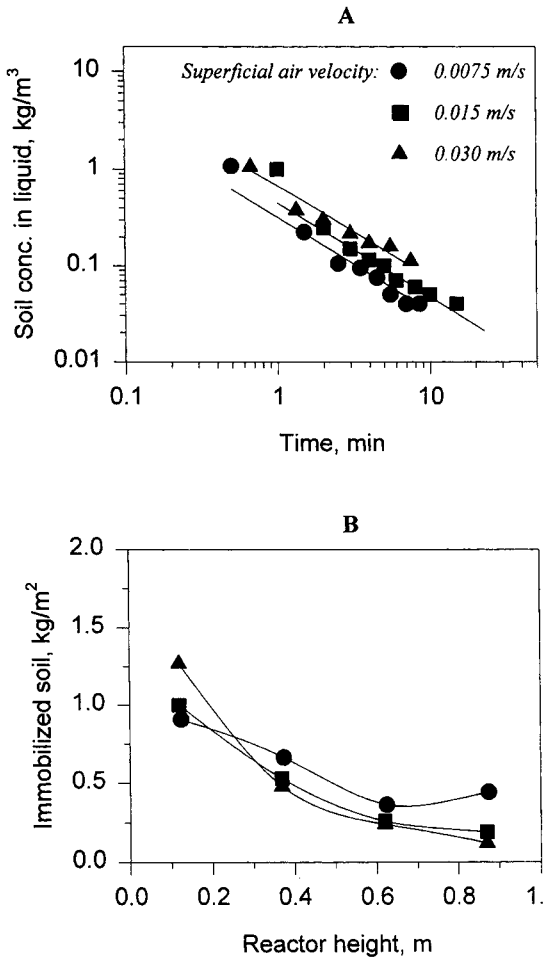

Figure 6. Effect of air flow rate on the process of soil immobilization.

The filtering device described earlier in this section was used in this study. The results of the experiments are shown in Figure 8. The existence of two different linear regions that seem to correspond to two mechanisms of soil-geotextile interaction was observed. The transition between both regions was observed at $\epsilon^3/(1-\epsilon)^2 = 8$, corresponding to a surface-soil density of 1.5 kg/m^2. Visually, a deposition of loose soil particles over the geotextile started at this point. This soil density is also close to the saturation soil density of 2.0 kg/m^2 (Figure 5). Therefore, the change in liquid permeability in the BC section in Figure 8 is due to the immobilization of solid particles and blocking the pores of the geotextile, while the change in the AB section is due to the formation of a fixed bed of solid particles over the surface of saturated geotextile. This result is used in the next section for the development of a mathematical model of the soil immobilization.

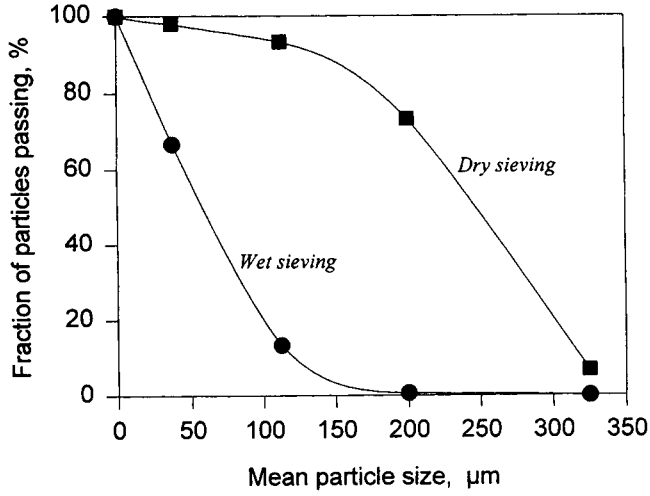

Figure 7. Comparison of the efficiency of dry and wet sieving of soil.

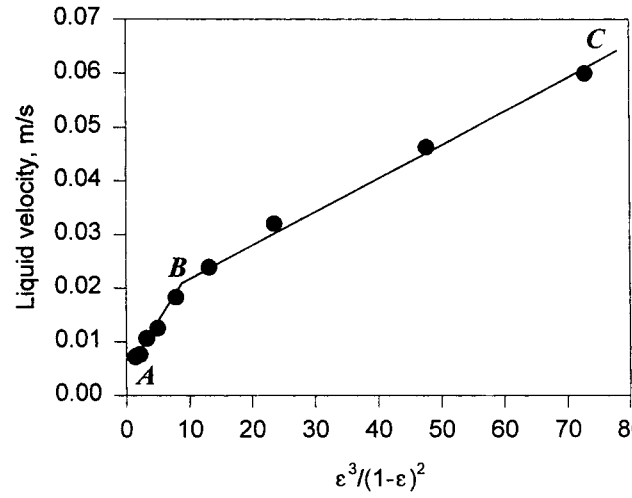

Figure 8. Change of liquid permeability as a function of the geotextile-immobilized soil porosity.

Mathematical Model of Soil Immobilization

The common characteristic of almost all the filters used in practice, particularly the deep-bed filters, is that they operate under close to plug-flow conditions. That is why the models of the process of deep-bed filtration are given as a function of the filter depth. One of the most popular kinetic models of the deep-bed filters is that of Iwasaki (1937):

$$\frac{dC}{dy} = -\lambda C, \tag{9}$$

where λ is the filter coefficient that varies with the particle accumulation. This model is valid for a clean filter, that is, at the initial moment of operation. Shekhtman (1961) proposed the following equation to account for the effect of particle deposition:

$$\lambda = \lambda_0(1-\beta\sigma), \tag{10}$$

where σ is the specific particle deposit.

Soil immobilization is in fact also a filtration process, but this filter is completely mixed due to the intensive liquid circulation (Karamanev et al., 1996a), and the process is in batch regime. Particle deposition is a function of both the vertical coordinate and time. In order to simplify the mathematical

model of the process, we now consider the particle deposition as a function of the vertical coordinate.

As already mentioned, the profile of the particle deposit is due to the profile of the horizontal liquid velocity by the reactor height. The higher velocity at the bottom of the reactor causes a greater particle deposition. This, in turn, decreases the liquid velocity. Therefore, a tendency toward flattening the horizontal liquid velocity profile with the height of the reactor is expected.

The vertical profile of horizontal liquid velocity in the ISBR can be related to the surface-soil density by replacing Δp with its equivalent (Eq. 3) in Eq. 8:

$$U_h = A \cdot (H_D - h) \cdot \frac{\epsilon^3}{(1-\epsilon)^2}, \tag{11}$$

where A is a coefficient of proportionality containing the constants in Eqs. 3 and 8. The relationships between the complex $(H_d - h)\epsilon^3/(1-\epsilon)^2$ and h based on the experimental data (Table 1) are shown in Figure 9. While there is some scatter, it can be assumed that the complex $(H_d - h)\epsilon^3/(1-\epsilon)^2$ (normalized by its mean value) is constant, and therefore the horizontal liquid velocity should also be nearly constant by the height of the reactor. The effect of the scatter of the complex $(H_d - h)\epsilon^3/(1-\epsilon)^2$ on the profile of soil concentration is not expected to be high, since this complex, respectively, the horizontal liquid velocity, is roughly proportional to the constant λ_0. These results suggest that a significant profile of the liquid velocity exists only for a short period after the introduction of the soil particles to the reactor, and after that it levels off. Since the deposition of soil particles with a certain size depends mainly on U_h, the solids deposition should also be constant (except in the initial period of immobilization). Therefore, the parameters σ and β in Eq. 10 can be assumed to be functions of time, but not of the vertical coordinate.

On the basis of the preceding findings and Eqs. 9 and 10, the following equation can be proposed for modeling the process of soil immobilization:

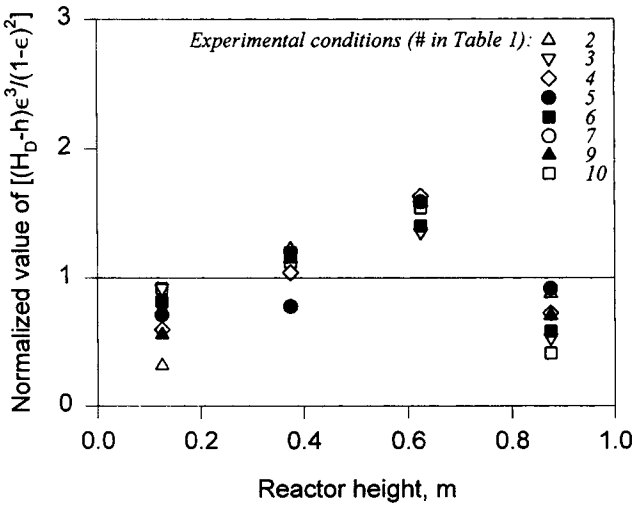

Figure 9. Complex $\epsilon^3/(1-\epsilon)^2$ as a function of the reactor height.

The complex was normalized by its mean value.

$$\frac{dC}{dt} = -\lambda_0 \left[1 - \beta\left(1 - \frac{C}{C_0}\right)\right] C. \tag{12}$$

Here we assumed that the specific particle deposit is proportional to the quantity of particles that disappeared from the liquid phase at time t, that is, $\sigma \sim (1 - C/C_0)$. After integration, the Eq. 12, gives

$$C = C_0 \frac{(1-\beta)}{\epsilon^{\lambda_0(1-\beta)t} - \beta}. \tag{13}$$

Our experimental data (Figures 3a, 5a, and 6a) were used to determine the constants λ_0 and β in Eq. 13 by a nonlinear regression. The solid lines in these figures represent the best-fit results. The values of the constants obtained are shown in Table 1. The values of β obtained were very close to unity for particle sizes above 200 μm. This is the range where the filtration effectiveness was close to unity (Figure 7). We assumed $\beta = 1$ for this particle size range. It has also been found that the constant λ_0 is inversely proportional to the initial concentration of soil in suspension (Figure 10). This result could be explained by the fact that $U_h \sim 1/(C_0 - C)$, and since $\lambda_0 \sim U_h$ and $C_0 \gg C$ at a later stage of the process, $\lambda_0 \sim 1/C_0$. Taking these results into account, Eq. 12 becomes a second-order kinetic model:

$$\frac{dC}{dt} = -\lambda_1 \left(\frac{C}{C_0}\right)^2, \tag{14}$$

where $\lambda_1 = \lambda_0/C_0$. Equation 14 can be easily integrated:

$$C = \frac{C_0^2}{C_0 + \lambda_1 t}. \tag{15}$$

It has to be stressed that this model is valid only for larger particles.

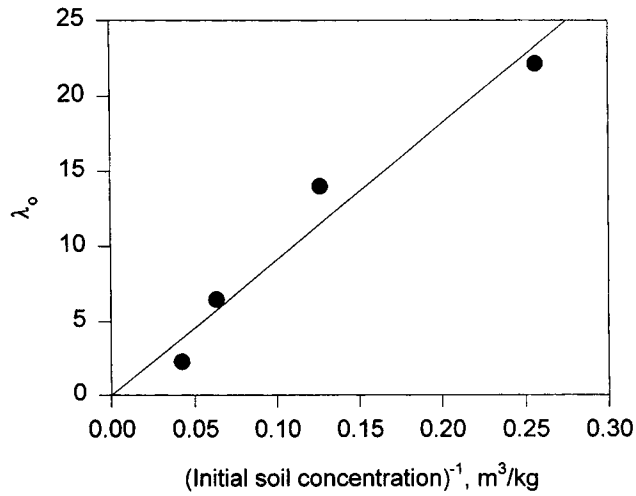

Figure 10. Effect of the initial slurry concentration on the filter coefficient.

Conclusions

The hydrodynamics of the soil immobilization process in a new type of bioreactor, the immobilized soil bioreactor, was studied. The effect of the main parameters such as particle size, gas flow rate, and the initial soil concentration on the dynamics of soil immobilization was studied. It was shown that increasing the gas flow rate and the initial soil concentration leads to a rise in the rate of immobilization. The immobilization was fastest at a mean particle size of 200 μm.

A mathematical model of the liquid flow structure in the reactor was proposed. This model explained the shape of the profile of surface-soil density by the height of the reactor. A model of the dynamics of soil immobilization was also developed on the basis of deep-bed filtration kinetics. It has been shown that the process of soil immobilization can be described by a second-order kinetic model when particle size was larger than 200 μm. This information will be useful for scaling up the reactor.

The applicability of the present results to different soil–geotextile systems has to be proven in further experiments, especially for the case of highly porous geotextiles that can be used for *in situ* biotreatment of groundwater.

Notation

A = constant (Eq. 11)
C = concentration of solids in suspension, kg/m^3
C_0 = initial solids concentration, kg/m^3
d_p = particle diameter, μm
g = gravity acceleration, m/s^2
U_{GR} = superficial velocity of gas in the riser, m/s
U_h = horizontal component of liquid velocity, m/s
y = vertical coordinate in deep-bed filtration, m
β = constant (Eq. 10)
ϵ_s = soil holdup in the immobilized soil structure
λ_0 = constant (Eq. 10)
λ_1 = constant (Eq. 14), kg/(m^3·s)
ρ = fluid density, kg/m^3

Literature Cited

Alexander, M., *Biodegradation and Bioremediation*, Academic Press, New York (1994).

American Society for Testing and Materials, *Standard Methods for Water Permeability of Geotextiles by Permittivity*, Standard D4491-92, Philadelphia (1992).

Atlas, R. M., "Bioremediation," *Chem. Eng. News*, **73**, 32 (1995).

Bird, R. B., W. E. Stewart, and E. N. Lightfoot, *Transport Phenomena*, Wiley, New York (1960).

Chisti, M. Y., *Airlift Bioreactors*, Elsevier, London (1989).

Christopher, B. R., and G. R. Fischer, "Geotextile Filtration Principles, Practices and Problems," *Geotex. Geomembr.*, **11**, 337 (1992).

Environmental Protection Agency, "Biotrol Soil Washing System for Treatment of a Wood Preserving Site. Applications Analysis," EPA publication 540A591003, Cincinnati, OH (1992).

Falyse, E., A. L. Rollin, J.-M. Rigo, and J.-P. Gourc, "Study of the Different Techniques Used to Determine the Filtration Opening of Geotextiles," *Proc. Can. Symp. on Geotextiles and Geomembranes*, Edmonton, Canada, p. 45 (1985).

Hills, J. H., "The Operation of a Bubble Column at High Throughputs. I. Gas Holdup Experiments," *Chem. Eng. J.*, **12**, 89 (1976).

Hsu, E. H., and L. T. Fan, "Experimental Study of Deep Bed Filtration: A Stochastic Treatment," *AIChE J.*, **30**, 267 (1984).

Iwasaki, T., "Some Notes on Sand Filtration," *JAWWA*, **29**, 159 (1937).

Ives, K. J., "Rapid Filtration," *Water Res.*, **4**, 201 (1970).

Karamanev, D. G., C. Chavarie, and R. Samson, "Hydrodynamics and Mass Transfer in an Airlift Reactor with a Semipermeable Draft Tube," *Chem. Eng. Sci.*, **51**, 1173 (1996a).

Karamanev, D. G., C. Chavarie, and R. Samson, "Pentachlorophenol Mineralization in an Immobilized Soil Bioreactor," World Congress of Chemical Engineering, San Diego, CA (1996b).

Orr, C., *Filtration: Principles and Practices*, Dekker, New York (1987).

Otte, M.-P., J. Gagnon, Y. Comeau, N. Matte, C. W. Greer, and R. Samson, "Activation of an Indigenous Microbial Consortium for Bioaugmentation of Pentachlorophenol/Creosote Contaminated Soils," *Appl. Microbiol. Biotechnol.*, **40**, 926 (1994).

Rigo, J. M., F. Lhote, A. L. Rollin, J. Mlynarek, and G. Lombard, "Influence of Geotextile Structure on Pore Size Determination," *Geosythetics: Microstructure and Performance, ASTM STP 1076*, I. D. Peggs, ed., American Society for Testing and Materials, Philadelphia, p. 90 (1990).

Shekhtman, Yu. M., *Filtration of Suspensions of Low Concentration*, USSR Academy of Sciences, Moscow (1961).

Silva, U., and S. K. Bhatia, "Filtration Performance of Geotextiles with Fine-Grained Soils," *Proc. Geosynthetics Conf.*, Vancouver, Canada, p. 483 (1993).

Tien, C., and A. C. Payatakes, "Advances in Deep Bed Filtration," *AIChE J.*, **25**, 737 (1979).

Manuscript received June 14, 1996, and revision received Dec. 19, 1996.